RF PULSE FLATTENING IN THE SWISSFEL TEST FACILITY BASED ON MODEL-FREE ITERATIVE LEARNING CONTROL*

Amin Rezaeizadeh†, Paul Scherrer Institut, Villigen, Switzerland
and Automatic Control Laboratory, ETH, Zürich, Switzerland
Thomas Schilcher, Paul Scherrer Institut, Villigen, Switzerland
Roy Smith, Automatic Control Laboratory, ETH, Zürich, Switzerland

Abstract

This paper introduces an iterative approach to producing flat-topped radio frequency (RF) pulses for driving the pulsed linear accelerators in the Swiss free electron laser (SwissFEL). The method is based on model-free iterative learning control which iteratively updates the input pulse shape in order to generate the desired amplitude and phase pulses at the output of the RF system. The method has been successfully applied to the klystron output to improve the flatness of the amplitude and phase pulse profiles.

INTRODUCTION

The SwissFEL project at PSI will develop a Free Electron Laser capable of generating extremely bright and short X-ray pulses [1]. The SwissFEL injector and linac RF drives operate in a pulsed mode at the rate of 100 Hz, using normal conducting RF accelerating structures. The input RF pulse length is relatively short (in the order of 1-3μs) and there is no RF digital feedback running within a pulse. In the two-bunch operating mode of the SwissFEL, each electron bunch is separated by 28 ns, and it is often required that the two bunches see the same amplitude and phase in the accelerating structure. To achieve this goal, an Iterative Learning Control (ILC) technique is introduced to generate a flat-topped (or generally any desired shape) RF pulse.

Iterative Learning Control is a method for controlling systems that operate in a repetitive, or trial-to-trial mode [2,3]. In this method, the measured trajectory is compared to the desired trajectory to give an error estimate which is then used to update the input for the next trial. A model-based ILC algorithm has been previously introduced in [4] which uses an intra-pulse state feedback and it has been implemented in several systems [5] including accelerators [6]. However, this approach is not applicable in the SwissFEL since no intra pulse digital feedback is feasible. A new version of ILC has been recently developed which is not based on the model of the system and thus the usual system identification procedure is not required [7]. The recent method has been modified and successfully tested on a C-band RF station in the SwissFEL test facility.

RF STATION LAYOUT

The RF and low-level RF layout of the SwissFEL C-band station is illustrated in Fig. 1. The discrete waveforms of the in-phase, I, and quadrature, Q, components of the RF signal are fed into the vector modulator to be up-converted to the carrier frequency (5.712GHz). Each waveform contains 2048 samples with the sampling time of $T_s = 4.2$ ns. The RF signal drives the klystron which delivers high power RF at the output. In C-band stations, an RF pulse compressor (Barrel Open Cavity) is placed after the klystron, followed by four accelerating structures.

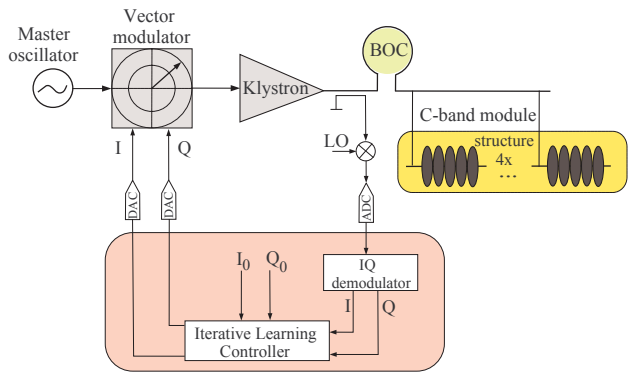

Figure 1: The RF layout of the SwissFEL C-band station.

For our experiment, we take the output of the klystron as the measured pulse whose shape is to be controlled. The signal is measured by a directional coupler and then down converted to the intermediate frequency (IF) of 39.67 MHz. The resulting signal is then sampled at the rate of 238 MHz, followed by a demodulation algorithm to obtain discrete waveforms of I and Q. The measured waveforms are compared to the desired ones and the ILC controller generates the next I and Q inputs to the DAC.

ITERATIVE LEARNING CONTROL SCHEME

The ILC is a technique to manipulate the input pulse shape iteratively until the output pulse shape fulfills the requirement. Model-free ILC methods are rarely investigated in literature, in contrast to a variety of model-based methods. Model-free ILC algorithms have the advantage that no system identification experiments are required. The idea behind our approach was developed by Janssens *et al.* [7].

Figure 2 illustrates the initial output signals of the klystron as a response to a rectangular input pulse. The colored area which is after filling time of the structures, denotes the region in which the electron bunches are fired. We refer to it as

* Work supported by Paul Scherrer Institut.
† aminre@ee.ethz.ch

ISBN 978-3-95450-133-5

the "flat-top" region, where ideally the pulse amplitude and phase should be constant.

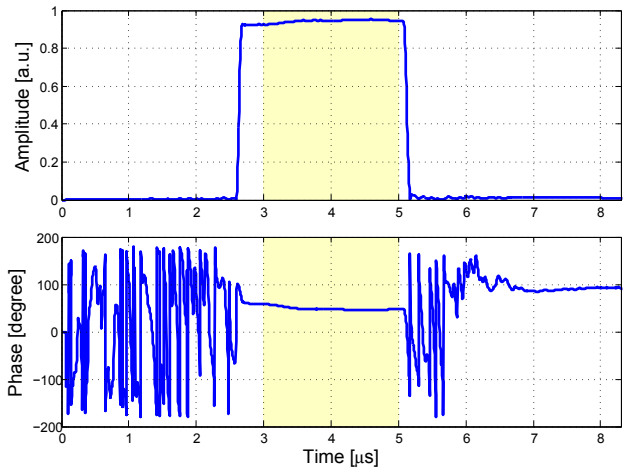

Figure 2: A typical pulse generated by the klystron. The measurement window consists of 2048 samples with sampling time of $T_s = 4.2$ ns. The electron-bunches are fired after filling time of the structures somewhere in the colored area, which we refer it to as the flat-topped region. The amplitude is normalized with respect to the saturation level (with 5% headroom).

For the notation throughout this paper, subscript i denotes the iteration counter, whereas index k captures the discrete time instants within one RF pulse. The following input update law is considered for an LTI SISO system,

$$u_{i+1}(k) = u_i(k) + u_{lc,i}(k) * \alpha_i(k), \tag{1}$$

where $u_i(k) \in \mathbb{R}$, $k \in \{1,2,...,N\}$, and $u_{lc,i}$ denotes any linear combination of the previous trials' input signals $u_0(k), u_1(k), ..., u_i(k)$, and where $\alpha_i(k)$ is a trial-varying but LTI FIR filter of length N. The asterisk denotes convolution. Since the system is assumed to be LTI, the corresponding output $y_{i+1}(k)$ is predicted to be

$$\hat{y}_{i+1}(k) = y_i(k) + y_{lc}(k) * \alpha_i(k), \tag{2}$$

where y_{lc} represents the corresponding linear combination of the previous trials' output signals $y_0(k), y_1(k), ..., y_i(k)$.

Equation 1 can be extended to MIMO systems by using the lifted system representation,

$$u_{i+1} = u_i + U_{lc}\tilde{\alpha}_i, \tag{3}$$

where

$$u_i := \begin{pmatrix} u_{Ii} \\ u_{Qi} \end{pmatrix}, \quad u_{Ii}, u_{Qi} \in \mathbb{R}^N,$$

and where,

$$u_{Ii} = \begin{pmatrix} u_{Ii}(1) \\ u_{Ii}(2) \\ \vdots \\ u_{Ii}(N) \end{pmatrix}, \quad u_{Qi} = \begin{pmatrix} u_{Qi}(1) \\ u_{Qi}(2) \\ \vdots \\ u_{Qi}(N) \end{pmatrix}, \tag{4}$$

and N denotes the number of samples in the flat-top region. Moreover,

$$U_{lc} = \begin{pmatrix} U_{lcI} & U_{lcQ} & \mathbf{0} & \mathbf{0} \\ \mathbf{0} & \mathbf{0} & U_{lcI} & U_{lcQ} \end{pmatrix}, \quad \tilde{\alpha}_i = \begin{pmatrix} \alpha_{IIi} \\ \alpha_{IQi} \\ \alpha_{QIi} \\ \alpha_{QQi} \end{pmatrix}$$

where U_{lcI} and U_{lcQ} denote the lower-triangular Toeplitz matrices of $u_{lcI}(k)$ and $u_{lcQ}(k)$, respectively.

A similar relationship can be derived for y,

$$\hat{y}_{i+1} = y_i + Y_{lc}\tilde{\alpha}_i, \tag{5}$$

where,

$$Y_{lc} = \begin{pmatrix} Y_{lcI} & Y_{lcQ} & \mathbf{0} & \mathbf{0} \\ \mathbf{0} & \mathbf{0} & Y_{lcI} & Y_{lcQ} \end{pmatrix},$$

and similarly, Y_{lcI} and Y_{lcQ} are the lower-triangular Toeplitz matrices of $y_{lcI}(k)$ and $y_{lcQ}(k)$, respectively.

Model-free ILC begins with the following optimization problem to determine the optimal filter $\tilde{\alpha}_i$,

$$\begin{aligned} \underset{\tilde{\alpha}_i}{\text{minimize}} \quad & \|\hat{y}_{i+1} - y_d\|_2^2 + r\|\tilde{\alpha}_i\|_2^2 \\ \text{subject to} \quad & \hat{y}_{i+1} = y_i + Y_{lc}\tilde{\alpha}_i \end{aligned} \tag{6}$$

where r is a weight on the input changes, and where y_d denotes the desired output vector which is expressed in terms of the desired I and Q waveforms:

$$y_d = \begin{pmatrix} y_{dI} \\ y_{dQ} \end{pmatrix} = \begin{pmatrix} a_d \cos\varphi_d \\ a_d \sin\varphi_d \end{pmatrix}, \tag{7}$$

where a_d and φ_d are respectively the desired output amplitude and phase trajectories in the flat-topped region (colored area in Fig. 2). We choose a smoothed amplitude trajectory as follows,

$$a_d(k) = a_0 e^{-(k-1)/k_0} + a_{ref}\left(1 - e^{-(k-1)/k_0}\right), \quad 1 \le k \le N, \tag{8}$$

where a_{ref} is the desired amplitude at the flat-top, and a_0 and k_0 are constants. A similar trajectory is defined for the phase. The reason for selecting such smooth trajectories is to avoid discontinuity which may result in large actuation to obtain flatness. The limits on the input signals are excluded from the constraints since they are inactive and can be treated separately.

As stated in [7], the following specific linear combination reduces the prediction error and allows Y_{lc} to be of full rank at every trial throughout the learning process,

$$U_{lc} = U_i - U_{i-1} + \gamma U_0, \tag{9}$$

and the linear combination matrix for the output would be

$$Y_{lc} = Y_i - Y_{i-1} + \gamma Y_0, \tag{10}$$

ISBN 978-3-95450-133-5

where γ is a tuning factor, and where U_i and U_0 are Toeplitz matrices of u_i and u_0, respectively, with u_0 denoting the initial input signal. Similar definitions apply for Y_i and Y_0.

The explicit solution to the optimization problem (6) can be readily calculated,

$$\tilde{\alpha}_i^* = (rI + Y_{lc}^T Y_{lc})^{-1} Y_{lc}^T (y_i - y_d). \quad (11)$$

Therefore, the input I and Q sequences are updated as

$$u_{i+1} = u_i + U_{lc}\tilde{\alpha}_i^*, \quad (12)$$

with defined bounds on the inputs.

EXPERIMENTAL RESULTS

As stated at the beginning, the control objective is to generate flat pulses at the klystron output. The actuation and measurement are based on I and Q waveforms, however we are mostly interested in amplitude and phase due to their physical meaning. Before running the ILC, the loop phase of the RF system was calibrated and set to zero, such that I and Q channels were approximately decoupled. Since the klystron is nonlinear with respect to amplitude, the inputs u_i are small signals around the operating point of the klystron. The algorithm begins with slightly exciting the input I and Q channels by small steps u_{I0} and u_{Q0}, respectively, which are constant over the whole pulse length.

Figure 3 shows the RF amplitude and phase waveforms after 30 iterations compared to the initial waveforms. The variance of the pulse over the flat-topped region is used as a measure of flatness. Figure 4 illustrates the standard deviation of the amplitude and phase pulses as the iteration advances. The iteration number "0" corresponds to the initial waveforms. The flatness has been improved by a factor of 3 and 5 for the amplitude and phase pulse, respectively. After around 20 iterations, the tracking error converges to the residual error which comes from the pulse to pulse noise through the system. The corresponding generated input waveforms are depicted in Fig. 5. As we can see, the resulting input signal is different from the nominal rectangular pulse.

SUMMARY

For multi-bunch operation of a pulsed mode FEL, in which several electron bunches are accelerated within an RF pulse, it is often required that the amplitude and phase remain constant over the pulse length so that the bunches achieve the same energy level. For pulsed mode machines, like the SwissFEL, where the pulse length is relatively short and no intra-pulse digital feedback is feasible, Iterative Learning Control is applicable to achieving the control objectives. In this paper, we investigated a model-free ILC approach and its application in RF pulse flattening of the klystron output. The proposed algorithm is applicable to RF waveform control in the other parts of the system, such as the RF pulse compressor and the Cavity pickups.

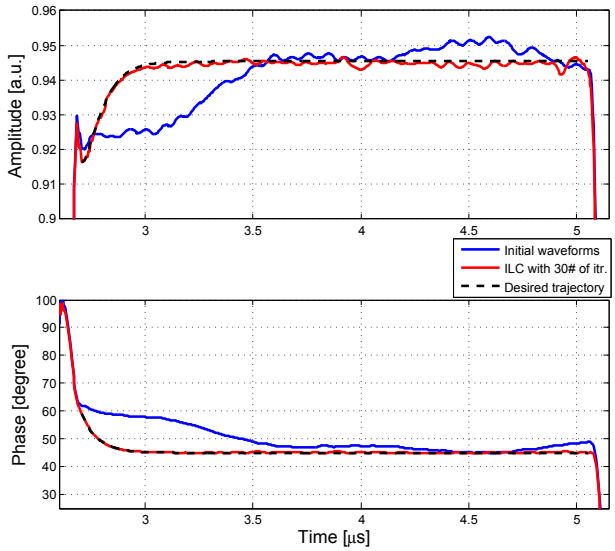

Figure 3: The klystron output amplitude and phase waveforms after 30 iterations (in red). The blue signal denotes the initial output waveforms (iteration #0).

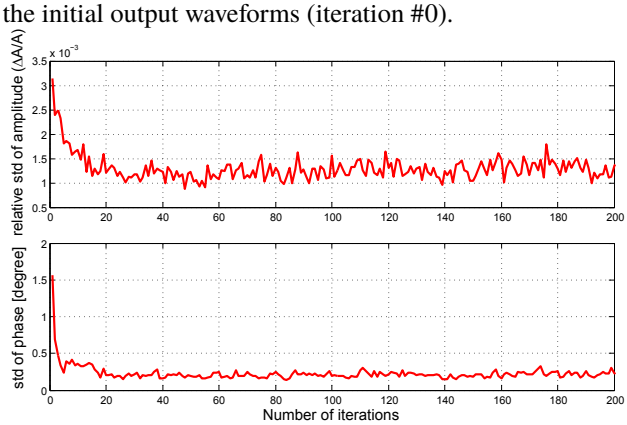

Figure 4: The standard deviation of flat-top amplitude and phase versus number of iterations.

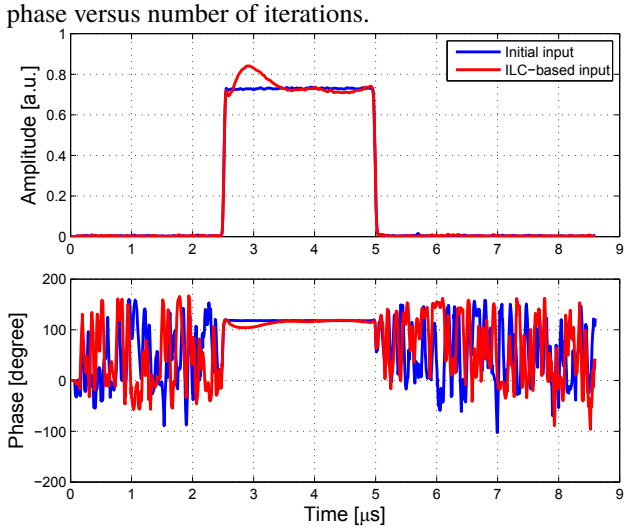

Figure 5: The input amplitude and phase waveforms generated by ILC (in red). The blue signal denotes the initial input waveforms (iteration #0).

ISBN 978-3-95450-133-5

ACKNOWLEDGMENT

The authors would like to thank the LLRF and the RF team who made this research possible, and special thanks goes to Roger Kalt for his help and support.

REFERENCES

[1] Romain Ganter et al., SwissFEL Conceptual Design Report, PSI, Villigen, Switzerland, 2010.

[2] M. Uchiyama, "Formulation of high-speed motion pattern of a mechanical arm by trial", *Trans. SICE (Society of Instrument and Control Engineers)*, vol.14, no. 6, pp.706-712, 1978 (in Japanese).

[3] D. A. Bristow et al. "A survey of iterative learning control", *IEEE Control Systems Magazine*, vol.26, no.3, pp.96–114, June 2006.

[4] N. Amann et al., "Iterative learning control using optimal feedback and feedforward actions", *International Journal of Control*, vol. 65, no. 2, pp.277–293., 1996.

[5] J.D. Ratcliffe et al., "Fast norm optimal iterative learning control for industrial applications", *American Control Conference, 2005. Proceedings of the 2005*, pp.1951–1956 vol. 3, 8-10 June 2005.

[6] S. Kichhoff et al., "An Iterative Learning Algorithm for Control of an Accelerator Based Free Electron Laser", *Proc. of the 47th IEEE Conference on Decision and Control*, Cancun, Mexico, Dec. 9-11, 2008.

[7] P. Janssens et al., "Model-free iterative learning control for LTI systems with actuator constraints", *Proc. of the 18th IFAC World Congress*, pp.11556-11561, Milano, Italy, August 28–September 2, 2011.

ISBN 978-3-95450-133-5